Tetragonal zinc-blende MnGa ultra-thin films with high magnetization directly grown on epi-ready GaAs(111) substrates

A. W. Arins, H. F. Jurca, J. Zarpellon, J. Varalda, I. L. Graff, A. J. A. de Oliveira, W. H. Schreiner, and D. H. Mosca

Citation: Appl. Phys. Lett. **102**, 102408 (2013); doi: 10.1063/1.4794951
View online: https://doi.org/10.1063/1.4794951
View Table of Contents: http://aip.scitation.org/toc/apl/102/10
Published by the American Institute of Physics

APPLIED PHYSICS LETTERS **102**, 102408 (2013)

Tetragonal zinc-blende MnGa ultra-thin films with high magnetization directly grown on epi-ready GaAs(111) substrates

A. W. Arins,[1] H. F. Jurca,[1] J. Zarpellon,[1] J. Varalda,[1] I. L. Graff,[1] A. J. A. de Oliveira,[2] W. H. Schreiner,[1] and D. H. Mosca[1]
[1]*Laboratório de Superfícies e Interfaces, Universidade Federal do Paraná, C. P. 19044 81531-990 Curitiba PR, Brazil*
[2]*Departamento de Física – Universidade Federal de São Carlos, Rodovia Washington Luiz, km 235, C. P. 676 13565-905 São Carlos SP, Brazil*

(Received 27 November 2012; accepted 26 February 2013; published online 12 March 2013)

We report on high quality MnGa epilayers directly grown on GaAs(111)-(1 × 1) reconstructed surface. MnGa layers are characterized by the stacking of (111) planes of tetragonal zinc-blende structure, which are rotated by 11° with respect to the underlying (111) planes of the GaAs lattice. These ultra-thin MnGa epilayers with lattice parameters $a = 0.55$ nm and $c = 0.61$ nm are stabilized for thickness between 5 and 20 nm with a net magnetic moment of 3.2 μ_B per Mn atom. These epilayers are potentially suited for semiconductor spintronics applications due to the reversal of its magnetization in relatively low magnetic fields. © *2013 American Institute of Physics*. [http://dx.doi.org/10.1063/1.4794951]

Manganese-gallium alloys grown on GaAs semiconductors by molecular beam epitaxy (MBE) are interesting candidates for applications in spintronics as spin injectors due to their thermodynamic stability, large spin polarization, square-like hysteresis loops, and large magnetic anisotropy.[1–7] Due to a rich phase diagram of the Mn-Ga system, several phases and compounds are found in films grown at different conditions.[8–13] Films of MnGa alloys are found at room temperature in the composition range of 49–76 at. % Mn adopting both $D0_{22}$- and $L1_0$-type structure,[8,12] with Curie temperatures above room temperature and magnetic moments as high as 2.5 μ_B per unit cell.[1,14] Electrical spin injection from δ-MnGa into a Ga(Al)As-based light-emitting diode was already demonstrated at remanence, without an applied magnetic field.[15] These compounds are therefore attractive for use in spin-valves, magnetic tunnel junction devices operating under perpendicular magnetic anisotropy, and spin injectors into semiconductors. Besides, MnGa alloys are also good candidates for producing materials suitable to replace some expensive rare-earth-based magnets in use today.[16] In this letter, we report on the MnGa epilayers directly grown on proper pregrowth treated epi-ready GaAs(111)B substrates. A well-defined epitaxial film-substrate relationship consistent with zinc-blende lattices and high magnetization is described below.

The experiments were performed in a custom-designed ultrahigh vacuum (UHV) MBE multichamber system, equipped with Ga and Mn effusion cells. Mn and Ga fluxes were measured using residual gas analyzer. The growth is monitored by reflection high energy electron diffraction (RHEED) and X-ray photoemission spectroscopy (XPS), which is performed using a VG Microtech ESCA3000 spectrometer equipped with a conventional Mg/Al X-ray source and a 250 mm hemispherical energy analyzer with an overall resolution of 0.8 eV at a 45° emission angle. Prior to MnGa growth, removal of the oxide layer of epi-ready GaAs(111)B commecial wafers at 580 °C was performed with a subsequent Ga exposure. RHEED pattern of a clean GaAs(111)B surface characterized by a (1 × 1) reconstruction is obtained. Several MnGa growth experiments were performed setting substrate temperatures at $T_s = 25$, 50, 150, or 250 °C, respectively, with an appropriate flux ratio R of Mn to Ga to achieve the specific stoichiometry in the films. For R between 1 and 2, the surface stoichiometry of the MnGa films varies from 52.5 to 60.0 at. % Mn, according to XPS performed *in situ*. Here we will describe our findings using the case with $R = 1.0$ and $T_s = 50$ °C. Under these conditions by opening Mn and Ga shutters during 24 min, MnGa layers with thicknesses of 5 nm were obtained after ramped up to 400 °C at 3 °C/min, and subsequent annealing during 30 min. Samples were also prepared under the same above-mentioned conditions with thicknesses of 10, 20, 25, and 50 nm. Samples thicker than 20 nm become (111)-textured with lower saturation magnetization values.

Figures 1(a)–1(c) show RHEED patterns measured along the respective [0$\bar{1}$1], [2$\bar{1}\bar{1}$], and [3$\bar{2}\bar{1}$] directions of the (1 × 1)-reconstructed surface of GaAs (111)B, as stabilized after removal of the oxide layer at 580 °C. Even the removal of the oxide layer being conducted at 580 °C and without an As flux to control the surface As concentration, it was observed that only a GaAs(111)B-(1 × 1) reconstruction was present, known as the $(1 \times 1)_{HT}$ phase.[17,18] RHEED patterns obtained from the MnGa layer cooled down to 50 °C after annealing are shown in Figures 1(d)–1(f). These RHEED patterns indicate high quality epitaxy of the MnGa layer with in-plane interplanar spacings quite similar to those of GaAs. The in-plane symmetry of MnGa layer is equivalent to that of GaAs(111)B surface. However, sharper RHEED patterns are systematically found shifted by approximately 11° off the angular positions corresponding to the [0$\bar{1}$1], [2$\bar{1}\bar{1}$], and [3$\bar{2}\bar{1}$] directions of GaAs. The in-plane interatomic distances of MnGa are, respectively, 0.343, 0.201, and 0.133 nm along the [0$\bar{1}$1], [2$\bar{1}\bar{1}$], and [3$\bar{2}\bar{1}$] directions of GaAs.

XRD experiments were performed in the X-ray power diffraction (XPD) beamline at the Brazilian synchrotron source (LNLS) to determine the epitaxial relationship of the MnGa layers with GaAs(111). Bragg peak corresponding to

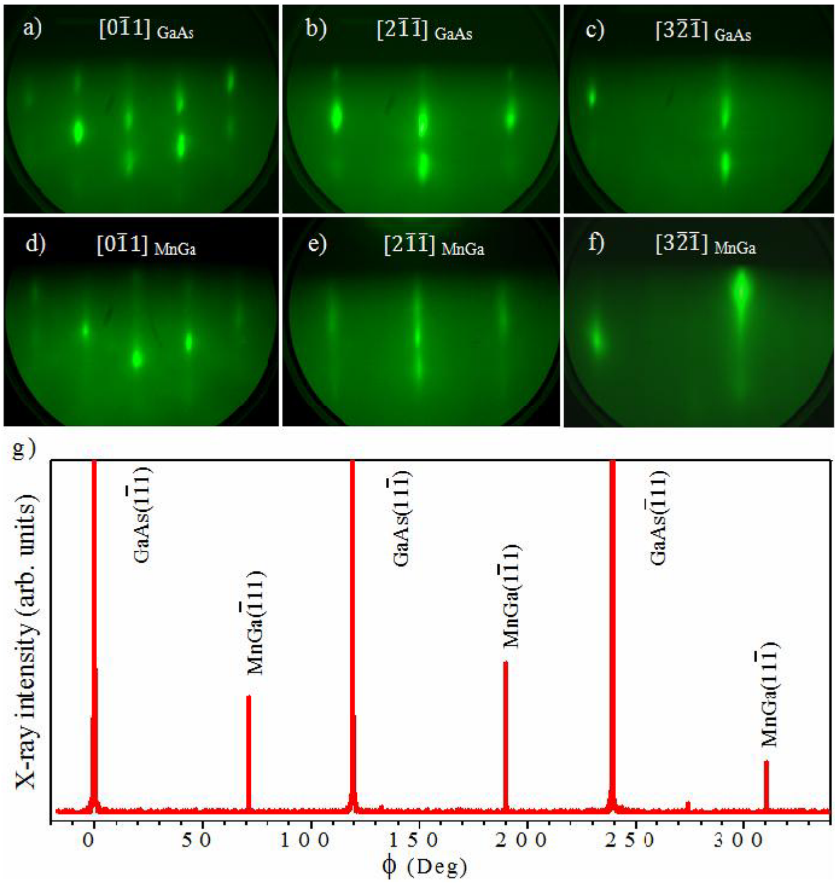

FIG. 1. RHEED patterns taken along the directions [0$\bar{1}$1], [2$\bar{1}\bar{1}$], and [3$\bar{2}\bar{1}$] of epi-ready GaAs(111)B substrates after removal of the oxide layer at 580 °C are, respectively, shown in (a), (b), and (c). RHEED patterns for the same directions of GaAs after the growth of MnGa epilayer are respectively shown in (d), (e), and (f). In panel (g) is shown the ϕ scan measured at room temperature for the MnGa epilayers by turning the film plane around the direction [1$\bar{1}$1] of the GaAs substrate, which is 70.5° off from the film normal.

(111) interplanar spacing of GaAs centered at $2\theta = 27.4°$ exhibit an adjacent Bragg peak assigned to (111) plane of MnGa with d = 0.327 nm. Figure 1(g) shows a ϕ scan obtained by turning the sample around the [1$\bar{1}$1] direction of the GaAs substrate at 70.5° from the film normal in order to evidence three diffraction peaks of the ⟨111⟩ family of directions. The Bragg diffraction peaks corresponding to GaAs(1$\bar{1}$1) planes are observed spaced by 120°. Diffraction peaks assigned to MnGa layer are also spaced by 120° but rotated by 71° (or 49°) relatively to diffraction peaks of GaAs. From the evaluation of both RHEED and XRD patterns is inferred an epitaxial relationship GaAs(111) // MnGa (111) along the normal to the films with each direction [0$\bar{1}$1], [2$\bar{1}\bar{1}$], and [3$\bar{2}\bar{1}$] of MnGa rotated by 11° with respect to the directions [0$\bar{1}$1], [2$\bar{1}\bar{1}$], and [3$\bar{2}\bar{1}$] of GaAs. These findings are consistent with a tetragonal zinc-blende (TZB) cell with $c = 0.61$ nm and $a = 0.55$ nm, which three-dimensional (3D) model is described below.

Figure 2(a) shows a body-centered cubic tetragonal (bct) cell for MnGa with lattice parameters $a' = 0.28$ nm and $c' = 0.31$ nm, as previously reported.[1,2] The bct cell is derived from two juxtaposed face-centered tetragonal (fct) cells of MnGa which preserves geometrical rules of a stable $L1_o$–type structure.[12] RHEED and XRD analyses are consistent with MnGa layer adopting TZB cell with $c = 0.61$ nm and $a = 0.55$ nm, as shown in Figure 2(b). Such TZB cell can be formed by assuming $c \approx 2c'$ and $a \approx 2a'$, which results from the stacking of bct(111) planes onto GaAs(111)B-(1 × 1) reconstructed surface. The overlaid model showing the epitaxial relationship between crystalline structures of TZB MnGa(111) and ZB GaAs(111) is illustrated in Figure 2(c). The rotation angles of 49° and 71° between lattices observed in Figure 1(g) can be obtained by a tetragonal distortion of about ∼2% in the ZB cell and rotation by 11° of MnGa lattice with respect to GaAs, confirmed by RHEED analyses. The schematic drawing of moiré pattern originated from the

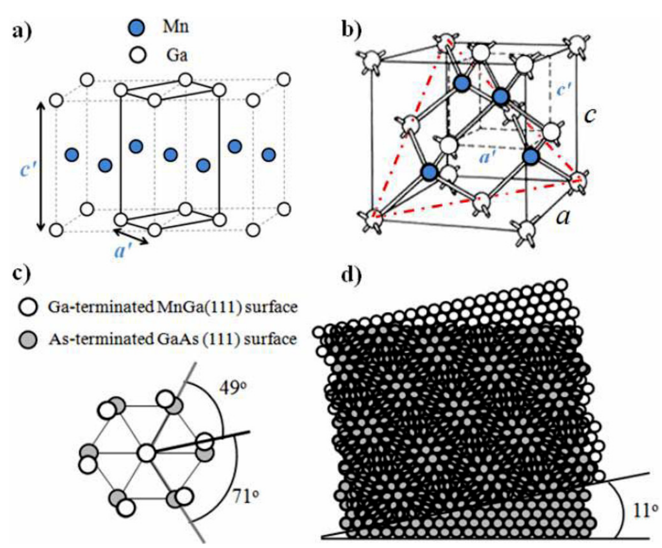

FIG. 2. (a) Perspective view of MnGa with $L1_o$ structure showing bct unit cell derived from two juxtaposed fct cells. (b) Tetragonal ZB crystal structure with dashed lines on top right corner indicating a bct subcell with the central lattice point occupied by Mn atom. Red dotted-dashed lines indicate (111) plane of the tetragonal ZB cell. (c) Ga/As-terminated (111) planes of MnGa/GaAs lattices are rotated by 11° one relative to the other. (d) Schematic drawing of moiré pattern created when two (111) lattice planes with slightly different interatomic distances are overlaid with an angle of 11° one relative to the other.

superposition of the (111) planes of these two slightly different ZB lattices is shown in Figure 2(d). The occurrence of this pattern implies a long range order with high coincidence of atoms of the two lattices, which by the way indicates a favorable in-plane epitaxial relationship. This 3D top view model correctly describes the accommodation of MnGa layer onto GaAs(111)B-(1 × 1) reconstructed surface with lattice parameters that are quite similar to those previously reported.[1,2] These TZB structure occurs for film thicknesses not exceeding 20 nm. Thicker MnGa films with 52.5–60.0 at. % Mn are (111)-textured even if annealed during longer time. The structural change leading to (111)-textured layers for thicknesses beyond 20 nm is not completely understood. According to atomic force microcopy analyses, when the film thickness increases from 5 to 20 nm the root-mean square surface roughness gradually increases from 2.5 to 7.4 nm for representative sampling areas of 5 μm × 5 μm. The basic forming process of the surface possibly initiates along the atomic terraces and evolves to the coexistence of different crystalline domains. However, the occupancy of surface sites due to the kinetic promoted by the annealing and diffusion processes of atoms of Ga and Mn deserves a more detailed investigation.

A vibrating sample magnetometer (PPMS Evercool II – Quantum Design) was used to characterize the magnetic properties of the epitaxial MnGa films as shown in Figure 3. The hysteresis loops shown in Figure 3(a) were measured at room temperature with magnetic field (H) applied out of the film plane and parallel to projections of *c* and *a* crystallographic axis in the film plane. The remanences (M_R) obtained with H along *c* and *a* are about 50% and 36% of saturation magnetization, respectively. Coercive fields (H_C) are about 210 Oe for both in-plane projections. Out-of-plane hysteresis loop exhibits low M_R ($\sim$6%) with $H_C = 110$ Oe. The saturation magnetization is $M_S = 650\ \text{emu/cm}^3$ which corresponds to 12.9 μ_B per TZB cell or 3.2 μ_B per Mn atom. Figure 3(b) shows the thickness dependence of the in-plane saturation magnetization. For layers containing 52.5 at. % Mn thicker than 20 nm it is observed a significant loss of magnetization. This is indicating that ordered TZB structure enables stabilize large values of saturation magnetization.

For films thinner than 20 nm the hysteresis loops measured with applied field along the directions denoted by H_1 and H_2 exhibit quite similar values of coercivity and saturation field. Despite of the significant differences in the remanent magnetization values, the in-plane anisotropy is weak, as shown in Figure 3(a). Out-of-plane magnetization saturates at fields as high as 40 kOe. This value is much higher than the shape anisotropy field estimated as $4\pi M_S \sim 8.2$ kOe. The Stoner-Wohlfarth approach can tentatively be used by admitting $2K/M_S \sim 40$ kOe, which yields an effective value of magnetic anisotropy $K \sim 1.3 \times 10^7\ \text{erg/cm}^3$. This effective value K is close to those reported for δ-MnGa alloys with 56–59 at. % Mn,[4] indicating that a strong magnetocrystalline anisotropy also occurs in our films. In δ-MnGa, the hybridization between the Mn *d* electrons and the delocalized Ga *p* electrons promotes a certain degree of itinerancy to the former, which favors an easy axis of magnetization along the crystallographic *c*-axis,[19] largely affected by strain.[14] In our TZB-MnGa, the in-plane magnetization is weakly anisotropic. The existence of equivalent epitaxial domains rotated by 120° one relative to the other should reduce the anisotropy of magnetization along *a* and *c* crystallographic axes. Due to a tetragonal distortion with $c/a \sim 1.1$ contributions of elastic and magnetoelastic anisotropy certainly play important roles in these TZB MnGa layers.

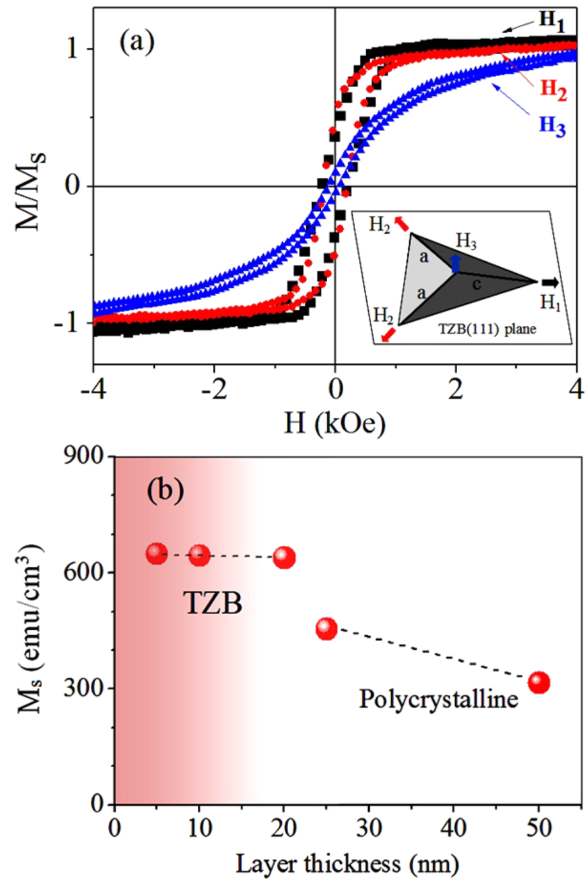

FIG. 3. (a) Hysteresis loops measured at room temperature with magnetic field applied along different crystallographic axes relative to TZB (111) plane of a MnGa epilayer grown on GaAs(111) substrate. The inset shows the crystallographic axes and magnetic field orientation used in the experiments with H_1 and H_2 lying in the film plane and H_3 along the film normal. (b) Thickness dependence of the saturation magnetization at 300 K for MnGa layers containing 52.5 at. % Mn.

The estimate value of 3.2 μ_B per Mn atom for tetragonally distorted ZB MnGa layers is higher than experimental values previously reported for bct cells of MnGa. For instance, magnetic moment values between 0.7 and 1.2 μ_B per Mn atom were reported by Tanaka *et al.*[1] and references therein, and 2.5 μ_B per Mn atom are found by Bedoya-Pinto *et al.*[8] Also, calculated values of 2.5 μ_B per Mn atom reported by Sakuma[19] and 2.8 μ_B per Mn atom described by Yang *et al.*[14] for strained bct cells are smaller than our present result. MnGa films with zinc-blend structure directly integrated on GaAs(111) certainly deserves further studies of their electronic structure in order to better understand the relation between the high magnetization and crystalline structure. Another important issue is the investigation of the possibility of matching between energy levels of TZB-MnGa and GaAs, which could favors the spin-injection efficiency for applications in spintronics devices. Our present results open approaches to explore the usage of these alloys as spin injectors in magnetic tunnel junctions.

In summary, we present results for MnGa epilayers directly grown on the (1×1)-reconstructed surface of GaAs(111)B substrates without GaAs buffer layer growth. We identify a heteroepitaxy between MnGa and GaAs with a well-defined epitaxial film-substrate relationship consistent with a zinc-blende lattice. Besides, noble-metal and rare-earth-free MnGa alloy films are interesting for applications in ultrahigh-density magnetic recording media Moreover, this kind of material is also promising to be developed for economical permanent magnets as pointed by Zhu *et al.*[20] The high saturation magnetization, together with moderate to low values of remanance and coercivity, make ZB MnAs suitable for spin injector electrodes in spintronics devices.

The authors thank Fabiano Yokaichiya (LNLS, Campinas) for excellent support and help during the XRD measurements and acknowledge financial support by CNPq, Fundação Araucária (Grant PRONEX 17386 #118/2010), and Brazilian Synchrotron Light Laboratory (LNLS) under proposal XPD-12533. Two of us thank CAPES/PRODOC (H.F.J) and REUNI/UFPR (J.Z.) for financial support.

[1] M. Tanaka, J. P. Harbison, J. DeBoeck, T. Sand, B. Philips, T. L. Cheeks, and V. G. Keramidas, Appl. Phys. Lett. **62**, 1565 (1993).
[2] M. Tanaka, Mater. Sci. Eng. B **31**, 117 (1995).
[3] W. Van Roy, H. Akinaga, S. Miyanishi, and K. Tanaka, Appl. Phys. Lett. **69**, 711 (1996).
[4] W. Van Roy, H. Akinaga, and S. Miyanishi, Phys. Rev. B **63**, 184417 (2001).
[5] K. M. Krishnan, Appl. Phys. Lett. **61**, 2365 (1992).
[6] W. Feng, D. V. Thiet, D. D. Dung, Y. Shin, and S. Cho, J. Appl. Phys. **108**, 113903 (2010).
[7] Z. Bai, Y. Cai, L. Shen, M. Yang, V. Ko, G. Han, and Y. Feng, Appl. Phys. Lett. **100**, 022408 (2012).
[8] A. Bedoya-Pinto, C. Zube, J. Malindretos, A. Urban, and A. Rizzi, Phys. Rev. B **84**, 104424 (2011).
[9] T. A. Bither and W. H. Cloud, J. Appl. Phys. **36**, 1501 (1965).
[10] F. Wu, S. Mizukami, D. Watanabe, H. Naganuma, M. Oogane, Y. Ando, and T. Miyazaki, Appl. Phys. Lett. **94**, 122503 (2009).
[11] E. Lu, D. C. Ingram, A. R. Smith, J. W. Knepper, and F. Y. Yang, Phys. Rev. Lett. **97**, 146101 (2006).
[12] H. Niida, T. Hori, H. Onodera, Y. Yamaguchi, and Y. Nakagawa, J. Appl. Phys. **79**, 5946 (1996).
[13] H. Kurt, K. Rode, M. Venkatesan, P. S. Stamenov, and J. M. D. Coey, Phys. Rev. B **83**, 020405 (2011).
[14] Z. Yang, J. Li, D. Wang, K. Zhang, and X. Xie, J. Magn. Magn. Mater. **182**, 369 (1998).
[15] C. Adelmann, J. L. Hilton, B. D. Schultz, S. McKernan, C. J. Palmstrøm, X. Lou, H.-S. Chiang, and P. A. Crowell, Appl. Phys. Lett. **89**, 112511 (2006).
[16] Editorial, Nat. Mater. **10**, 157 (2011).
[17] J. M. C. Thornton, D. A. Woolf, and P. Weightman, Surf. Sci. **380**, 548 (1997).
[18] J. M. C. Thornton, D. A. Woolf, and P. Weightman, Appl. Surf. Sci. **123–124**, 115 (1998).
[19] A. Sakuma, J. Magn. Magn. Mater. **187**, 105 (1998).
[20] L. Zhu, S. Nie, K. Meng, D. Pan, J. Zhao, and H. Zheng, Adv. Mater. **24**, 4547 (2012).